

ORIGINAL
RESEARCH

C.-H. Lu
H.-L. Chen
W.-N. Chang
N.-W. Tsai
H.-C. Wang
T.-M. Yang
Y.-J. Lin
C.-P. Lin
C.-C. Chen
B.-C. Cheng
W.-C. Lin



Assessing the Chronic Neuropsychologic Sequelae of Human Immunodeficiency Virus–Negative Cryptococcal Meningitis by Using Diffusion Tensor Imaging

BACKGROUND AND PURPOSE: The high rate of neuropsychologic sequelae in CM survivors indicates that initial antifungal therapy is far from being satisfactory. This prospective cross-sectional study applied DTI on HIV-negative CM patients to determine whether microstructural changes in brain tissue are associated with subsequent cognitive symptoms.

MATERIALS AND METHODS: Fifteen patients with HIV-negative CM and 15 sex- and age-matched healthy volunteers were evaluated and compared. All underwent complete medical and neurologic examinations and neuropsychologic testing. Brain DTI was obtained to derive the FA and ADC of several brain regions. Correlations among DTI parameters, neuropsychologic rating scores, and cryptococcal-antigen titer in CSF were analyzed.

RESULTS: Significant ADC values increased and FA values decreased in HIV-negative CM patients in multiple selected regions of interest, including the genu of the corpus callosum and the frontal, parietal, orbito-frontal, and periventricular white matter and lentiform nucleus. Higher CSF cryptococcal-antigen titer on admission was associated with poorer DTI parameters ($r = -0.666$, $P = .018$), which were linearly related to worse cognitive performance during follow-up.

CONCLUSIONS: The decline in brain DTI parameters in the associated brain areas indicates an HIV-negative CM microstructural pathology that is related to neuropsychologic consequences.

ABBREVIATIONS: ADC = apparent diffusion coefficient; CASI = Cognitive Ability Screening Instrument; CM = cryptococcal meningitis; CNS = central nervous system; DTI = diffusion tensor imaging; DWI = diffusion-weighted MR imaging; FA = fractional anisotropy; HIV = human immunodeficiency virus; MANCOVA = multivariate analysis of covariance; ROI = region of interest; WAIS = Wechsler Adult Intelligence scale; WM = white matter

CM is the most common life-threatening opportunistic fungal meningitis. It is an especially important cause of morbidity and mortality among immunocompromised patients.¹⁻⁴ Although antifungal therapy has been introduced, the high rate of neurologic sequelae among survivors indicates that therapy for CM is far from being satisfactory.⁵⁻⁷

New nonconventional MR imaging techniques such as DWI have been proposed as tools to improve diagnostic accuracy and achieve a better understanding of the pathophysiology and psychology of the diseased brain.^{8,9} DTI, a DWI technique, provides a quantitative noninvasive method for delineating anatomic integrity, particularly for

the WM pathways, by measuring the extent and direction of diffusion. FA values indicate WM directionality and fiber coherence, whereas ADC indicates the degree of diffusion restriction or cellular attenuation.¹⁰ By measuring FA and ADC values, decreased myelin integrity or neuron cell loss is reportedly associated with cognitive impairment in normal aging,¹¹ degenerative disease,¹² psychiatric disorders,¹³ and even CNS toxicity.¹⁴ DTI also has been assessed to quantify periventricular WM changes in neonatal meningitis,¹⁵ and decreased FA values are observed in patients with abnormal outcome.

Furthermore, the dilated Virchow-Robin spaces in cryptococcal invasion suggest possible microstructure injury in the basal ganglia. Currently, there has been no prospective study investigating DTI techniques in HIV-negative CM patients. The effect of structure alteration on the neuropsychologic decline in this particular group is unknown. Increasing the understanding of cognitive impairment that occurs in such patients may help improve treatment strategies.

The primary objective of the current study is to test the hypothesis that changes of DTI parameters in the basal ganglia and in vulnerable WM, such as the periventricular region, occur in HIV-negative CM patients during long-term follow-up. The secondary objective is to examine the relationship between anatomic deficits and cognition, as assessed by standard neuropsychologic testing.

Received October 11, 2010; accepted after revision November 26.

From the Departments of Neurology (C.-H.L., W.-N.C., N.-W.T.), Radiology (H.-L.C., W.-C.L.), Neurosurgery (H.-C.W., T.-M.Y., Y.-J.L.), Psychiatry (C.-C.C.), and Medicine (B.-C.C.), Chang Gung Memorial Hospital-Kaohsiung Medical Center, Chang Gung University College of Medicine, Kaohsiung, Taiwan; Department of Biological Science (C.-H.L.), National Sun Yat-Sen University, Kaohsiung, Taiwan; and Department of Biomedical Imaging and Radiological Sciences (H.-L.C., C.-P.L., W.-C.L.), National Yang-Ming University, Taipei, Taiwan.

This study was supported by grants from the Chang Gung Memorial Hospital (CMRPG870991) and was approved by the hospital's Institutional Review Committee on Human Research.

Please address correspondence to Wei-Che Lin, Department of Radiology, Chang Gung Memorial Hospital, 123, Ta Pei Rd, Niao Sung Hsiang, Kaohsiung Hsien, Taiwan; e-mail: u64lin@yahoo.com.tw

Indicates article with supplemental on-line tables.

DOI 10.3174/ajnr.A2489

Materials and Methods

Subjects

From March to May 2010, 28 HIV-negative CM patients with discontinued antifungal therapy, discharged from the hospital for >3 months, were seen at the Neurology Outpatient Clinic of Chang Gung Memorial Hospital-Kaohsiung Medical Center. Chang Gung Memorial Hospital CGMH-Kaohsiung is a 2482-bed acute-care teaching hospital that provides primary and tertiary referral care and is the largest medical center in southern Taiwan. Of these patients, 15 were enrolled in this study and received both neuroimaging and neuropsychologic follow-up examination. The hospital's Institutional Review Committee on Human Research approved the study, and all patients provided written informed consent.

CM was defined as either 1) isolation of *Cryptococcus neoformans* in one or more CSF cultures, positive CSF cryptococcal antigen titer, or positive CSF India ink and clinical features of meningitis; or 2) isolation of *C. neoformans* in blood culture with clinical presentations of meningitis and typical CSF features. It is our practice to arrange brain MR imaging study immediately after hospitalization as well as before discharge from the hospital. Furthermore, repeat CT and/or MR imaging was obtained if there was clinical deterioration before discharge. Hydrocephalus was diagnosed by the presence of a dilated temporal horn of the lateral ventricle, without obvious brain atrophy, and/or an Evan ratio of >0.3 on CT or MR imaging during admission. Evan ratio is the ratio of the ventricular width of the bilateral frontal horn to the maximal biparietal diameter.¹⁶

CM patients were excluded if they had any of the following: 1) age <20 years or >75 years; 2) evidence of alcoholism or any other addictive disorders, or known affective or other psychiatric disease and use of sedatives or neuroleptics; and 3) known neurologic disorders potentially affecting the CNS, or severe recent life events that may interfere with neuropsychologic testing. Of the 13 excluded patients, 9 had severe neurologic sequelae that could interfere with neuropsychologic testing and 4 were hesitant to enroll in the study.

All of the included patients underwent complete medical and neurologic examinations, and neuropsychologic testing. Neurologists integrated the clinical manifestations and neuropsychologic findings. For comparison, 15 sex- and age-matched healthy subjects without a medical history of neurologic disease and with similar lengths of school education were recruited through advertising within the hospital and served as the control group.

MR Imaging Acquisition

All our patients received MR imaging within 3 days after hospitalization, and these 15 patients underwent both MR imaging and DTI study between March and May 2010. The mean interval between first MR imaging (MR imaging during acute phase but without DTI study) and first including both MR imaging and DTI studies was 60.5 ± 39.6 months. For initial evaluation on admission and follow-up, MR imaging was performed by using a 3T unit (Signa Excite HD; GE Medical Systems, Milwaukee, Wisconsin). All sections were acquired along the anterior/posterior commissure plane, which was ensured by a multiplanar T1-weighted localizer image before each study. Axial T1-weighted images, axial T2-weighted images, and T1-weighted enhanced images were acquired to evaluate intracranial lesions.

DTI Data Acquisition

During follow-up, DTI datasets were acquired by using single-shot diffusion spin-echo, echo-planar imaging with a TR/TE of 15 800

millisecond/minimum, a 2.5-mm section, a matrix of 128×128 , number of excitations of 3, and a FOV of 25.6×25.6 cm, yielding an in-plane resolution of 2 mm, with a total acquisition time of 12 minutes. DTI encoding entailed 13 noncollinear directions with $b = 1000$ s/mm² and a nondiffusion T2-weighted image. Contiguous sections ($n = 55$) were obtained without an intersection gap to achieve total cerebral coverage.

The DTI sets were transferred to an off-line workstation for further analysis by the FuncTool diffusion tensor protocol (Advanced Workstation 4.2; GE Healthcare), which contained a preprocessing function to remove echo-planar imaging distortions, including scaling, shearing, and translation due to eddy current effects from diffusion gradient. The distortion-corrected data were then interpolated to attain isotropic voxels and decoded to obtain the tensor field for each voxel. The algorithm computed each pixel location the 6 coefficients of the diffusion tensor. The tensor field data were then used to compute the DTI metrics, including the mean diffusivity (ADC) and FA for each voxel.

Neuropsychologic Testing

A clinical psychologist blinded to the patients' exposure status performed the neuropsychologic tests. Subjects completed a test battery assembled to assess executive function, attention, and memory. Neuropsychologic evaluation was performed by using subtests of WAIS-III.¹⁷ These included information that measured general knowledge, digit span, vocabulary ability to define 35 words, arithmetic, letter-number sequencing, comprehension, similarities, picture completion, matrix reasoning, block design, picture arrangement, digit symbol, and object assembly. The subtests of vocabulary, similarities, and general knowledge yielded the verbal comprehension; picture completion, block design, and matrix reasoning yielded the perceptual reasoning; and arithmetic, digit span, and letter-number sequencing yielded the working memory.

CASI¹⁸ was obtained in all subjects. The CASI, developed as a brief screening cognitive assessment test for comparative studies in Asian and American populations, had 9 domains of cognitive function (ie, attention, concentration, orientation, short- and long-term memory, language ability, visual construction, word list generation, abstraction, and judgment), with scores ranging from 0 (worst) to 100 (best). The mean cognitive scores for measures of neuropsychologic testing were generated by averaging the standardized data from verbal comprehension, perceptual reasoning, working memory of WAIS, and the CASI. Mean cognitive scores were applied for further correlation by DTI parameters.

ROI Analysis of DTI Data

The MR imaging findings in CNS cryptococcosis included abnormal dilated Virchow-Robin spaces, cryptococcomas, abnormal leptomeningeal enhancement, hydrocephalus, and focal gray matter and WM lesions.¹⁹⁻²² Meningitis also could lead to periventricular WM injury by glial cell infiltration.¹⁵ The spectrum of abnormalities on MR imaging reflected potential anatomies of fungal invasion. Based on these reports, several major WM and deep gray matter areas were selected for ROI analysis (Fig 1).

A radiologist measured the ROIs, 50–100 mm² depending on the anatomic region, which were confirmed by another radiologist to avoid malpositioning. All ROI analyses were conducted on DTI-derived maps, including the null image (b value = 0) and their corresponding color-coded FA maps to ensure exact anatomic locations. The regions where ROIs were placed appeared normal on conven-

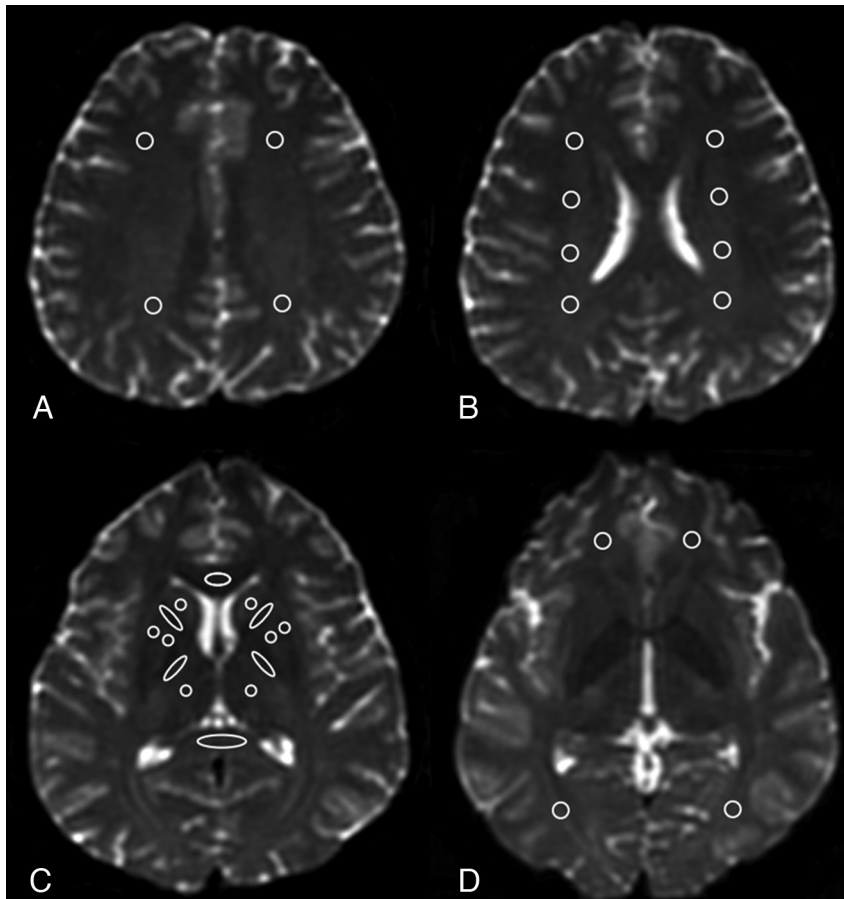


Fig 1. Location of the ROIs in a healthy control. *A*, WM of the high frontal and parietal lobes located anterior and posterior to the central sulcus on the most caudal section on which they were visible and on the following cranial section. *B*, Periventricular WM was measured on the subsequent caudal section. *C*, ROIs at the genu and splenium of the corpus callosum were placed on 3 consecutive sections. The anterior and posterior internal capsules, caudate nucleus, globus pallidus, putamen, and thalamus were measured on 2 contiguous sections. *D*, Orbito-frontal WM was placed on the most caudal section of the lateral ventricles. Occipital-lobe ROIs were placed in the optic radiations of 2 contiguous sections, starting from the most caudal section on which the occipital horn of the lateral ventricle was imaged. Temporal lobe WM ROIs were placed lateral to the temporal horn of the lateral ventricle (not shown).

tional MR imaging and were fixed a priori in all patients as well as in controls. These measurements were performed according to the methods described in previous studies.^{14,15,23}

In WM analysis, ROIs were placed on the genu and splenium of the corpus callosum; the anterior and posterior limbs of the internal capsule; and the subcortical orbito-frontal, high frontal, parietal, occipital, temporal, and periventricular WM. For deep gray matter analysis, ROIs of the caudate nucleus, globus pallidus, putamen, and thalamus were selected. Raters were blinded to the subjects' details, and the ADC and FA for the 24 brain areas were measured.

Statistical Analysis

First, the age and education level between the 2 patient groups were analyzed by using the Student *t* test. Sex difference was analyzed by χ^2 test or the Fisher exact test, where appropriate. The neuropsychologic test scores between patients and control subjects were estimated by 1-way analysis of covariance model with the participant age and sex as covariates. Statistical differences in the DTI parameters of each ROI between the 2 groups were estimated by MANCOVA model, with the participant age and sex as covariates. The MANCOVA model was defined by one between-subject factor and 24 ROIs as dependent variables, with multiple comparison collection (Bonferroni correction). Secondary partial correlation analyses (2-tailed) between non-parametric tests and DTI parameters showing differences between the 2 groups were performed, controlling for age and sex.

High CSF cryptococcal antigen was reportedly associated with poor outcome and high prevalence of cryptococcal-related intracranial lesions.⁵ Cognitive impairment, as a CM complication, has previously been attributed to hydrocephalus and elevated intracranial pressure in HIV subjects.²⁴ Last the partial correlation test was chosen to examine the relationship between CSF cryptococcal antigen and declining DTI parameters, controlling for age, sex, and ventricle size (Evan ratio). Statistical significance was defined at $P < .05$. All statistical analyses were performed by using the SPSS software, version 10.0 (SPSS, Chicago, Illinois).

Results

Baseline Characteristics and Imaging Findings of Study Patients

The baseline characteristics of all subjects are listed in On-line Table 1. Neuroimaging findings and CSF cryptococcal-antigen titers of the 15 patients on admission and follow-up CT and/or MR imaging are listed in On-line Table 2. Two radiologists carefully evaluated all of the images. Baseline CT and MR were normal in 2 of the 15 patients. The 4 major MR imaging manifestations in the remaining 13 patients were meningeal/gyral enhancement (60%), basal ganglia infarction/Virchow-Robin spaces dilation (47%), hydrocephalus (33%), and focal cerebritis (27%). The mean interval between

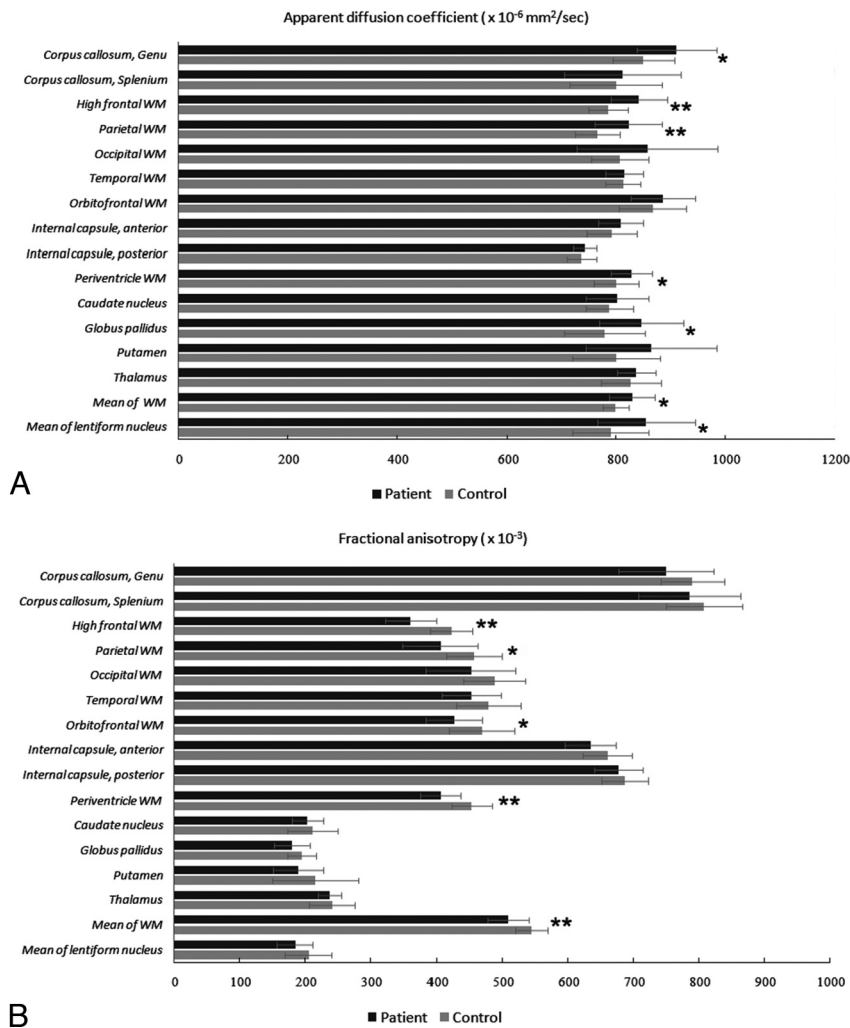


Fig 2. ADC (A) and FA (B) values measured with DTI. * $P < .05$; ** $P < .01$.

hospital discharge and follow-up was 59.8 months (range, 3–122 months).

During follow-up, interval evolutions of image studies were compared lesion by lesion. The absence of brain lesions was recorded and defined as disappearance of the hyperintensity on T2-weighted image without any increased enhancement. There was resolution of the imaging abnormality in 8 of the 13 patients. There was resolution of the imaging abnormality in 8 of the 13 patients and persistent abnormality in the other 5 patients (On-line Table 2).

Neuropsychologic Testing

Results of each WAIS-III and CASI subtest are presented in On-line Table 1. Patients scored lower—digit span and block design tests of WASI, indicating deficits in attention, concentration, and visuo-spatial skills.²⁵ Patients also exhibited poorer abstract thinking in the CASI than the healthy controls, suggesting an executive function defect. Patients experienced poor performance compared with the controls on 2 major WAIS components, perceptual reasoning and working memory index, and on CASI test scores. The mean cognitive scores derived from the above-mentioned tests also revealed significantly poor cognitive outcome in CM patients. In general, the

trend in means for the individual tests indicated that survivors of HIV-negative CM showed global impairment even after a 5-year follow-up.

ADC

The MANCOVA revealed significant difference between the 2 groups on ADC value ($F = 3.763, P = .011$). Comparisons between HIV-negative CM patients and controls showed that patients had increased ADC in the genu of the corpus callosum (910.8 ± 73.4 versus 850.5 ± 56.9 ; $F = 6.308, P = .018$), high frontal (841.8 ± 51.7 versus 785.6 ± 36.7 ; $F = 11.780, P = .002$), parietal (822.8 ± 61.6 versus 766.4 ± 41.4 ; $F = 8.673, P = .006$), periventricular (828.6 ± 38.0 versus 800.2 ± 40.8 ; $F = 5.127, P = .032$), and globus pallidus areas (846.0 ± 77.1 versus 779.5 ± 74.3 ; $F = 5.772, P = .023$). The ADC of the overall measured WM ($F = 6.010, P = .021$) and lentiform nucleus ($F = 4.983, P = .034$), made up of the globus pallidus and putamen, was also significantly increased (Fig 2).

FA

The MANCOVA revealed significant difference between the 2 groups on FA value ($F = 2.650, P = .048$). Among HIV-negative CM patients, FA was significantly reduced compared

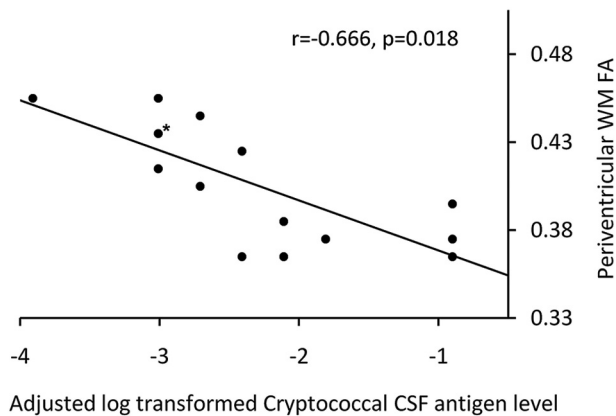


Fig 3. Relationship between log-transformed cryptococcal CSF antigen titer level and FA value in the periventricles after adjustments for age, sex, and Evan ratio in 15 CM patients (asterisk, 2 dots were overlapped).

with controls in the high frontal (360.9 ± 38.1 versus 422.9 ± 31.7 ; $F = 23.522$, $P < .001$), parietal (405.8 ± 56.9 versus 457.0 ± 42.0 ; $F = 7.862$, $P = .009$), orbito-frontal (426.9 ± 42.9 versus 468.9 ± 50.2 ; $F = 6.086$, $P = .020$), and periventricular WM (406.3 ± 30.5 versus 453.1 ± 31.0 ; $F = 17.359$, $P < 0.001$). The FA of the overall measured WM ($F = 12.182$, $P = .002$) likewise significantly decreased (Fig 2), whereas the FA was reduced in HIV-negative CM patients in regions with abundant WM, such as the anterior and the posterior limbs of the internal capsule and the temporal and occipital WM. However, the differences were not significant. In the deep gray matter, the FA also was reduced compared with the controls but not statistically significant.

Relationship between DTI Parameters and Neuropsychologic Function

Relation between ADC and Cognitive Domains. Decreased digit span scores were negatively associated with ADC value in the globus pallidus ($\gamma = -0.374$, $P = .046$). Decreased perceptual reasoning index was inversely associated with ADC value in the parietal ($\gamma = -0.415$, $P = .025$) and periventricular WM ($\gamma = -0.392$, $P = .036$). Scores of abstract thinking were negatively associated with the genu corpus callosum ADC value ($\gamma = -0.368$, $P = .050$), whereas lower mean cognition scores were inversely associated with periventricular ADC value ($\gamma = -0.375$, $P = .045$).

Relation between FA and Cognitive Domains. Worse digit span scores, lower working memory index, and poorer mean cognition scores correlated with decreased FA values in the high frontal ($\gamma = 0.404$, $P = .030$; $\gamma = 0.414$, $P = .026$; and $\gamma = 0.435$, $P = .018$, respectively), orbito-frontal ($\gamma = 0.408$, $P = .028$; $\gamma = 0.431$, $P = .019$; and $\gamma = 0.405$, $P = .029$, respectively), and mean WM ($\gamma = 0.467$, $P = .001$; $\gamma = 0.402$, $P = .031$; and $\gamma = 0.372$, $P = .047$, respectively).

Relationship between DTI Declines and CSF Cryptococcal-Antigen Titer

Elevated CSF cryptococcal-antigen titer on admission was negatively associated with lower FA value in the periventricular region ($r = -0.666$, $P = .018$) on follow-up in CM patients (Fig 3). Otherwise, there was no significant correlation be-

tween CSF antigen titer and ADC value in either the WM or the deep gray matter.

Discussion

Survivors of bacterial meningitis often complain of neurologic²⁶ and neuropsychologic sequelae.²⁷ Cognitive deficiencies after bacterial and viral meningitis (predominantly short-term and working memory) also have been described.²⁸ Although impaired cognition related to CM infection, ranging from acute confusion, psychosis, and mania to encephalopathy, is well known, evidence is based on case reports²⁹⁻³² or comorbidity with HIV infection.³³ This is the first study to show correlations between neuropsychologic sequelae and changes in DTI parameters in patients with HIV-negative CM by measuring DTI parameters. The study also confirms the hypothesis that anatomic integrity subsequently decreases in the chronic phase of the disease, even after antimicrobial therapy, and that CSF antigen titers can predict the degree of DTI parameter degradation. Furthermore, the degree of decline of DTI parameters correlates well with cognitive outcomes.

Cryptococcosis is often seen in patients with compromised cellular immune response, particularly in AIDS patients. However, up to 30% of cases are in patients with no predisposing condition, such as the patient group in this study.³⁴ Patients with higher lactate concentration, lower glucose concentration, CSF cryptococcal antigen titer above 1:1024, positive India ink preparation, and presence of hydrocephalus and seizure show significantly worse outcomes.^{5,35} Thus, they require prompt treatment.

Sadly, neuropsychologic sequelae in patients with low risk factors are easily overlooked. A significant proportion of CM survivors can develop various neurologic sequelae, including cognitive impairment.³⁵ The current patient group does not have adverse factors but apparently has good recovery, though they still show more frequent pathologic results than the control group for all domains examined. Large numbers of patients with cognitive impairment will therefore continue to have complaints attributable to their illness after the acute phase of the disease.

Meningitis can lead to brain atrophy, with loss of cortical neurons and periventricular WM injury by glial cell infiltration.¹⁵ Most active cryptococcal neuroradiologic lesions regress, with residual gliosis found in few patients after 5 years of follow-up. Although WM changes might occur due to microangiopathy in some aging subjects after long-time follow up, and might be unrelated to the disease process, diffusely decreased FA in normal-appearing parenchyma in patients is consistent with a previous neuropathologic study.³⁶

Inflammation, ischemia, and oxidative stress are considered responsible for the development of WM injury after meningitis.^{15,36} From conventional MR imaging, only 2 of the 15 patients in the initial study and 2 of the 15 patients in the follow-up study had parietal lobe encephalitis. No one has frontal or periventricular lesions. However, there was significant microstructural damage in parietal WM observed in residual patients (FA, $P = .002$; ADC, $P = .013$) after excluding patients with pre-existing lesions.

In contrast, 10 of 15 patients with lepto-meningeal enhancements and/or hydrocephalus suggest intense inflammation. Selective WM degradation implies that the leading cause

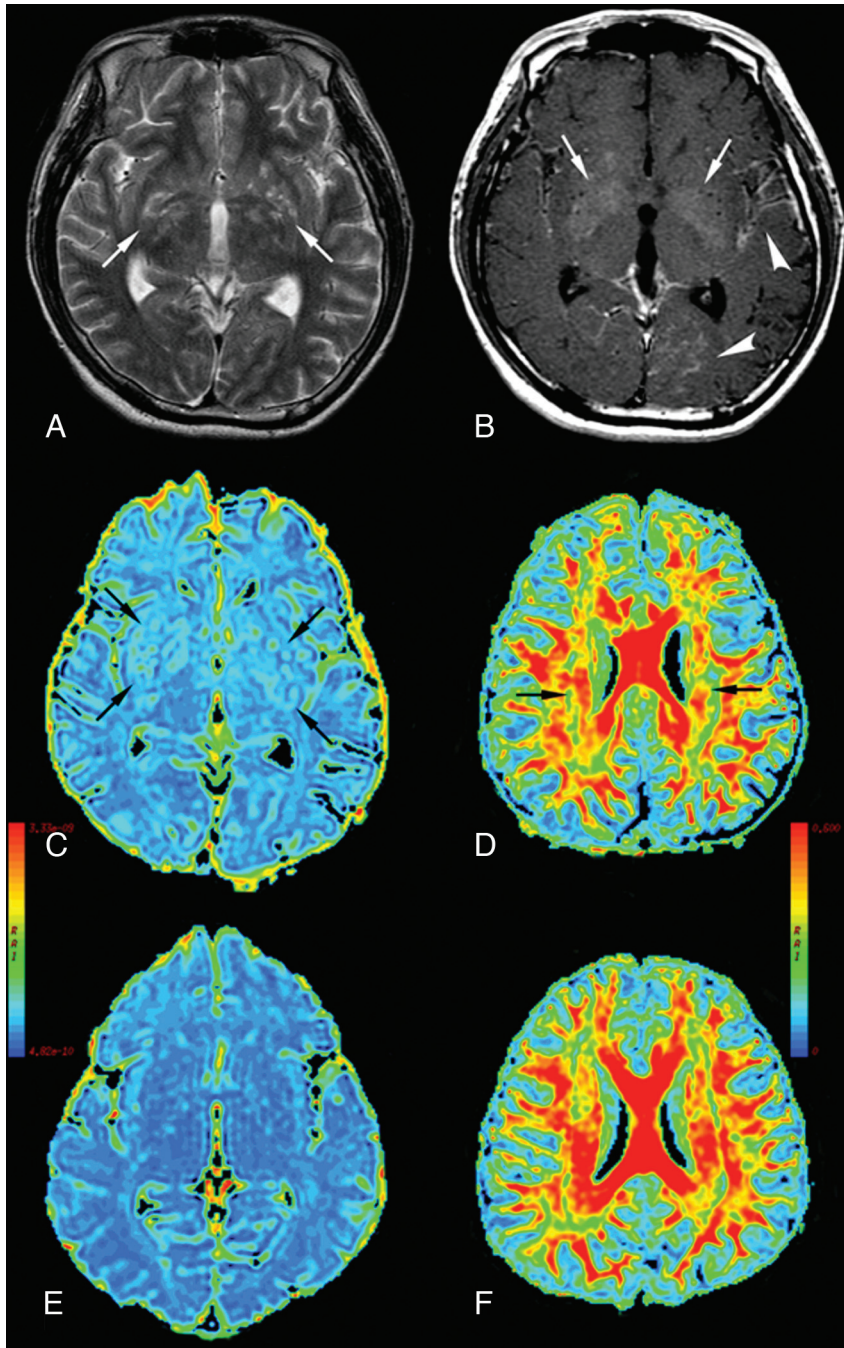


Fig 4. A 31-year-old man with CM (A–D) and a healthy control (E and F). A, Axial T2-weighted image. B, Axial T1-weighted image with contrast infusion displaying bilateral lentiform nucleus (arrows), left temporal and left occipital meningeal enhancement (arrowheads). C, ADC maps displaying bilateral dilated Virchow-Robin spaces (arrows) in the lentiform nucleus, and global cerebral ADC value increased. D, periventricular white matter FA value decreased (arrows).

of outcome is mixed or complicated. In CM, inflammation is initially confined to the subarachnoid space and is prone to infiltrating the Virchow-Robin perivascular spaces. Thromboembolic results from vasculitis within small perivascular spaces further lead to tissue ischemia by decreasing cerebral perfusion. The frontal, parietal, and periventricular WM have relatively few oligodendrocytes to maintain heightened numbers of axons. Oxidative stress during the ischemic condition amplifies pathologic processes due to the high metabolic demands of oligodendrocytes.¹⁴

Hydrocephalus is a common complication in the CM

group. Hydrocephalus after CM may compromise brain vessels and lead to brain ischemia and consciousness deterioration. Based on admission MR imaging, 5 patients had signs of hydrocephalus. However, several studies point to the lack of radiologic hydrocephalus in cases of high opening CSF pressure.⁷ In patients with acute hydrocephalus, obvious decreased FA and increased ADC are found in the corpus callosum³⁷ because it is the tissue most affected by enlarged ventricles (because it is located just above them) and therefore degenerates more rapidly. Studies on the pathology of the corpus callosum in acute and chronic states, and of the periven-

tricular system in cases of chronic hydrocephalus, support this.^{38,39} There is also sustained leptomeningeal enhancement and nonresolved hyperintensity from follow-up MR imaging in some of the patients. Despite the absence of strong imaging evidence of hydrocephalus, an insidious, chronic arachnoiditis can exist. Prolonged elevated ventricle pressure impairs myelin repair (Fig 4), which is further confirmed by results here.

The obvious increase in ADC value in the lentiform nucleus is not surprising. The Virchow-Robin spaces appear as the main anatomic sites involved, even radiologically during cerebral cryptococcosis.²⁰ The cryptococcal organisms spread from the basal cisterns through the Virchow-Robin spaces, dilating these spaces, to ultimately propagate in the lentiform nucleus. Such lesions have been described as characteristic for cryptococcosis, which show these lesions to be small cystic collections of cryptococcal organisms. The T2-weighted image sequences are more sensitive in detecting these lesions compared with CT or T1-weighted MR images.¹⁹ The high microbial burden in the perivascular space causes small arterial infarction and venous thrombosis. Both cause cell death and gliosis. Neuronal loss, as well as fungal cyst accumulation, alters ADC values (Fig 4).

Conclusions

This study supplements previous MR imaging studies by adding a level of anatomic detail to the relationship between changes in diffusion parameters and cognitive dysfunction. It also demonstrates that high fungal burden, based on high antigen titers, correlates to periventricular WM injury in CM. Although the results are based on a relatively small cohort, the strength of the clinical MR imaging correlations highlights the importance of widespread pathology in CM, which suggests that quantifying tissue damage may improve the capacity to monitor the neuropsychologic consequences of CM.

References

- Zuger A, Louie E, Holzman RS, et al. Cryptococcal disease in patients with the acquired immunodeficiency syndrome. Diagnostic features and outcome of treatment. *Ann Intern Med* 1986;104:234–40
- Hellmann DB, Petri M, Whiting-O'Keefe Q. Fatal infections in systemic lupus erythematosus: the role of opportunistic organisms. *Medicine* 1987;66:341–48
- Kaplan MH, Rosen PP, Armstrong D. Cryptococcosis in a cancer hospital: clinical and pathological correlates in forty-six patients. *Cancer* 1977;39:2265–74
- Khanna N, Chandramuki A, Desai A, et al. Cryptococcal infections of the central nervous system: an analysis of predisposing factors, laboratory findings and outcome in patients from South India with special reference to HIV infection. *J Med Microbiol* 1996;45:376–79
- Lu CH, Chang WN, Chang HW, et al. The prognostic factors of cryptococcal meningitis in HIV-negative patients. *J Hosp Infect* 1999;42:313–20
- Lan SH, Chang WN, Lu CH, et al. Cerebral infarction in chronic meningitis: a comparison of tuberculous meningitis and cryptococcal meningitis. *QJM* 2001;94:247–53
- Liliang PC, Liang CL, Chang WN, et al. Shunt surgery for hydrocephalus complicating cryptococcal meningitis in human immunodeficiency virus-negative patients. *Clin Infect Dis* 2003;37:673–78
- Eric Searls D, Sico JJ, Bulent Omay S, et al. Unusual presentations of nervous system infection by *Cryptococcus neoformans*. *Clin Neurol Neurosurg* 2009;111:638–42
- Patro SN, Kesavadas C, Thomas B, et al. Uncommon presentation of intracranial cryptococcal infection mimicking tuberculous infection in two immunocompetent patients. *Singapore Med J* 2009;50:e133–37

- Jellison BJ, Field AS, Medow J, et al. Diffusion tensor imaging of cerebral white matter: a pictorial review of physics, fiber tract anatomy, and tumor imaging patterns. *AJNR Am J Neuroradiol* 2004;25:356–69
- Moseley M. Diffusion tensor imaging and aging—a review. *NMR Biomed* 2002;15:553–60
- Buschert V, Bokde AL, Hampel H. Cognitive intervention in Alzheimer disease. *Nat Rev Neurol* 2010;6:508–17
- Lim KO, Helpert JA. Neuropsychiatric applications of DTI—a review. *NMR Biomed* 2002;15:587–93
- Lin WC, Lu CH, Lee YC, et al. White matter damage in carbon monoxide intoxication assessed in vivo using diffusion tensor MR imaging. *AJNR Am J Neuroradiol* 2009;30:1248–55
- Malik GK, Trivedi R, Gupta A, et al. Quantitative DTI assessment of periventricular white matter changes in neonatal meningitis. *Brain Dev* 2008;30:334–41
- Greenberg MS. Hydrocephalus. In: Greenberg MS, ed. *Handbook of Neurosurgery*, 4th ed. Lakeland, Florida: Greenberg Graphics; 1997:571–600
- Wechsler D. *Wechsler Adult Intelligence Scale*, revised. New York: Psychological Cooperation; 1981
- Lin KN, Wang PN, Liu CY, et al. Cutoff scores of the cognitive abilities screening instrument, Chinese version in screening of dementia. *Dement Geriatr Cogn Disord* 2002;14:176–82
- Tien RD, Chu PK, Hesselink JR, et al. Intracranial cryptococcosis in immunocompromised patients: CT and MR findings in 29 cases. *AJNR Am J Neuroradiol* 1991;12:283–89
- Wehn SM, Heinz ER, Burger PC, et al. Dilated Virchow-Robin spaces in cryptococcal meningitis associated with AIDS: CT and MR findings. *J Comput Assist Tomogr* 1989;13:756–62
- Takasu A, Taneda M, Otuki H, et al. Gd-DTPA-enhanced MR imaging of cryptococcal meningoencephalitis. *Neuroradiology* 1991;33:443–46
- Olsen WL, Longo FM, Mills CM, et al. White matter disease in AIDS: findings at MR imaging. *Radiology* 1988;169:445–48
- Bozzali M, Falini A, Franceschi M, et al. White matter damage in Alzheimer's disease assessed in vivo using diffusion tensor magnetic resonance imaging. *J Neurol Neurosurg Psychiatry* 2002;72:742–46
- Graybill JR, Sobel J, Saag M, et al. Diagnosis and management of increased intracranial pressure in patients with AIDS and cryptococcal meningitis. The NIAID Mycoses Study Group and AIDS Cooperative Treatment Groups. *Clin Infect Dis* 2000;30:47–54
- Groth-Marnat G, Teal M. Block design as a measure of everyday spatial ability: a study of ecological validity. *Percept Mot Skills* 2000;90:522–26
- Durand ML, Calderwood SB, Weber DJ, et al. Acute bacterial meningitis in adults. A review of 493 episodes. *N Engl J Med* 1993;328:21–28
- Bohr V, Rasmussen N, Hansen B, et al. Pneumococcal meningitis: an evaluation of prognostic factors in 164 cases based on mortality and on a study of lasting sequelae. *J Infect* 1985;10:143–57
- Schmidt H, Heimann B, Djukic M, et al. Neuropsychological sequelae of bacterial and viral meningitis. *Brain* 2006;129:333–45
- Sa'adah MA, Araj GF, Diab SM, et al. Cryptococcal meningitis and confusional psychosis. A case report and literature review. *Trop Geogr Med* 1995;47:224–26
- Ala TA, Doss RC, Sullivan CJ. Reversible dementia: a case of cryptococcal meningitis masquerading as Alzheimer's disease. *J Alzheimers Dis* 2004;6:503–08
- Rafael H. Secondary Alzheimer started by cryptococcal meningitis. *J Alzheimers Dis* 2005;7:99–100; author reply 101
- Hoffmann M, Muniz J, Carroll E, et al. Cryptococcal meningitis misdiagnosed as Alzheimer's disease: complete neurological and cognitive recovery with treatment. *J Alzheimers Dis* 2009;16:517–20
- Gumbo T, Kadzirange G, Mielke J, et al. *Cryptococcus neoformans* meningoencephalitis in African children with acquired immunodeficiency syndrome. *Pediatr Infect Dis J* 2002;21:54–56
- Dismukes WE. Management of cryptococcosis. *Clin Infect Dis* 1993;17(suppl 2):S507–12
- Diamond RD, Bennett JE. Prognostic factors in cryptococcal meningitis. A study in 111 cases. *Ann Intern Med* 1974;80:176–81
- Lee SC, Dickson DW, Casadevall A. Pathology of cryptococcal meningoencephalitis: analysis of 27 patients with pathogenetic implications. *Hum Pathol* 1996;27:839–47
- Assaf Y, Ben-Sira L, Constantini S, et al. Diffusion tensor imaging in hydrocephalus: initial experience. *AJNR Am J Neuroradiol* 2006;27:1717–24
- Del Bigio MR, Wilson MJ, Enno T. Chronic hydrocephalus in rats and humans: white matter loss and behavior changes. *Ann Neurol* 2003;53:337–46
- Ding Y, McAllister JP 2nd, Yao B, et al. Axonal damage associated with enlargement of ventricles during hydrocephalus: a silver impregnation study. *Neurol Res* 2001;23:581–87